Diabetes-associated MYT1 and MYT3 regulate human β-cell insulin secretion and survival via other diabetes-risk genes

Ruiying Hu[1], Mahircan Yagan[1], Yu Wang[2], Xin Tong[3], Nala Hamilton[1], Teri D. Doss[3], Jinhua Liu[3], Yanwen Xu[1,4], Alan J. Simmons[1,4], Ken S. Lau[1,4], Roland Stein[3], Irina Kaverina[1], Katie C. Coate[3, 5, 6], Qi Liu[2], and Guoqiang Gu[1,*]

1 Department of Cell and Developmental Biology, Vanderbilt University School of Medicine, Nashville, TN 37232, USA.

2 Department of Biostatistics and Center for Quantitative Sciences, Vanderbilt Medical Center, Nashville, TN 37232, USA.

3 Department of Molecular Physiology and Biophysics, Vanderbilt University School of Medicine, Nashville, TN 37232, USA.

4 Center for Computational Systems Biology, Epithelial Biology Center, Vanderbilt University School of Medicine, Nashville, TN 37232, USA.

5 Department of Medicine, Vanderbilt University Medical Center, Nashville, TN, 37232, USA

6 Department of Veterans Affairs, Tennessee Valley Healthcare System, Nashville, TN, USA.

*: Corresponding author: Guoqiang.gu@vanderbilt.edu (ORCRID: 0000-0003-0772-9139)

Word counts: 3,989.

Author Emails:

Ruiying Hu: Ruiying.hu@vanderbilt.edu

Mahircan Yagan: Mahircan.Yagan.hu@vanderbilt.edu

Yu Wang: Yu.wang.2@VUMC.org

Xin Tong: xin.tong.sci@gamil.com

Nala Hamilton: Helen.hamilton@vanderbilt.edu

Teri D. Doss: Teri.d.stevenson@vanderbilt.edu

Jinhua Liu: Jin-hua.liu@vanderbilt.edu

Yanwen Xu: yanwen.xu@vanderbilt.edu

Alan J. Simmons: Alan.j.simmons@vanderbilt.edu

Ken S. Lau: Ken.s.lau@vanderbilt.edu

Roland Stein: Roland.stein@vanderbilt.edu

Irina Kaverina: Irina.kaverina@vanderbilt.edu

Katie C. Coat: Katie.coate@VUMC.org

Qi Liu: Qi.liu@VUMC.org

Guoqiang Gu: Guoqiang.gu@vanderbilt.edu

Abstract

Genetic and environmental factors together cause islet β-cell failure, leading to Type 2 diabetes (T2D). Yet how they integrate to regulate β-cells remains largely unclear. Here, we examined how two members of the Myelin transcription factor family (MYT1, 2, and 3) prevent human β-cell failure under obesity-related stress. We have reported that obesity-related nutrient levels induce these factors. They prevent β-cell failure in mouse islets and human β-cell lines. Their variants are all associated with human T2D, and their downregulation accompanies β-cell dysfunction. By knocking down *MYT1* or *MYT3* separately in primary human donor islets, we show here that they have overlapping but distinct functions. Under normal culture conditions, MYT1-knockdown (KD) causes β-cell death, while MYT3-KD compromises glucose-stimulated insulin secretion. Under obesity-induced metabolic stress *in vivo*, MYT3-KD also causes β-cell death. Accordingly, these TFs regulate common and unique genes, with MYT1-KD de-regulating several genes in cell death and Ca^{2+} binding, while MYT3-KD de-regulating genes involved in mitochondria, ER, etc. Intriguingly, the MYT1 and MYT3-regulated genes are enriched for T2D-associated genes. These findings suggest that the MYT TFs complement each other to serve as a node that integrates genetic and environmental factors to prevent β-cell failure and T2D.

Research in Context

It is now known that:

- All MYT TFs (including MYT1, 2, 3) are associated with the risk of T2D, and their downregulation accompanies β-cell failure during human T2D development.
- Obesity-related high glucose/free fatty acids regulate the levels and/or nuclear localization of MYT1 and MYT3 in primary human β-cells, implying them as integrators of genetic and nutrition factors to determine the risk of β-cell failure and T2D.
- Myt TFs, via coregulators including Sin3, work together to prevent postnatal β-cell failure in mice and the death of a human β-cell line, suggesting they are essential switches for β-cell protection.

The key remaining question is:

- How do these TFs regulate primary human β-cell failure in response to different nutritional signals?

Our new findings are:

- Reduced MYT1 or MYT3 expression levels in primary human islets via knockdown compromised β-cell survival or secretion, respectively, under normal physiology.
- MYT3-knockdown compromises human β-cell survival in obesity.
- MYT1/MYT3-regulated genes are enriched for those associated with T2D risk.

Impact:

- Manipulating MYT TF activities, via modulating their associations with coregulators, could be explored to attenuate β-cell failure and risk of T2D.

Introduction

Both genetic predisposition and non-genetic influence contribute to type 2 diabetes (T2D). To this end, hundreds of genetic loci have been associated with T2D risk (1). Most of these loci can predispose β cells to dysfunction, loss of identity, or death (i.e., β-cell failure) (2). Environmental factors can exacerbate this failure by overwhelming β-cells with a heavy workload or stressor molecule accumulation (3). How β-cells integrate these factors to prevent this failure remains largely unknown.

A significant risk factor for β-cell failure is obesity, which can induce insulin resistance in the fat, liver, and skeletal muscle so that higher insulin levels are needed for blood glucose homeostasis (4-6). To compensate, β-cells increase insulin output in circulation. However, sustained high insulin output can exhaust the β-cells due to the stress-producing nature of insulin secretion (5,7). Specifically, high levels of glucose metabolism will promote insulin biosynthesis, co-producing unfolded proinsulin in the endoplasmic reticulum (ER) that, when reaching high levels, induces ER stress and dysfunction (8). In addition, high glucose and free fatty acid metabolism in β-cells produce reactive oxygen species (ROS) and/or toxic lipid metabolites (9). These products, at high levels, cause oxidative stress and mitochondrial dysfunction while also exacerbating ER stress. Henceforth, β-cells activate unfolded protein response (UPR) and/or oxidative stress response (OSR) to clean up these stressor molecules (10,11). If properly controlled, the overall result of these responses is proteostasis and sustainable β-cell function. However, overactivation of stress responses can overly reduce essential β-cell proteins or activate proapoptotic genes (4,12). Thus, both the inactivation and overactivation of stress responses (i.e., maladaptation) need to be avoided for sustained β-cell function (13).

The myelin transcription factor [Myt (in mice) or MYT (in human) TF] family consists of three zinc finger proteins that are expressed in neuronal and endocrine cells [Myt TFs, including *Myt1 (Nzf2)*, *Myt2 (Myt1L, Nzf1)*, and *Myt3 (St18, Nzf387)*]. They can serve as both transcriptional repressors or activators in a context-dependent fashion via association with co-regulators SIN3 or LSD1 (14,15). In humans, single-nucleotide polymorphisms (SNPs) and deletion mutations in any of the three are associated with human diseases, including mental illness and diabetes (1,16-20). Intriguingly, our recent studies showed that the expression of these factors in mice was enhanced by obesity-related stress *in vivo* (21). Their level reduction or elimination in mice compromised β-cell function, proliferation, or death (21-23), likely via induction of maladaptation (24-27). More importantly, this mechanism appears conserved in human β-cells. Specifically, the protein levels and/or nuclear localization of MYT1/MYT3 were regulated by glucose and free fatty acids in primary human β-cells (21). The reduced MYT TF production positively correlated with human β-cell dysfunction during the development of T2D (21). Co-knockdown (KD) of all three factors compromised the viability of a human β-cell line while inducing the transcription of several stress response genes (21).

The above studies establish the Myt TFs as environment-responsive regulators that prevent stress-induced mouse β-cell failure. However, the specific functions of these factors in human β-cells remain unknown since the co-KD of these factors leads to cell death, preventing more detailed characterization of the mutant cells. This study's primary goal is to examine the roles of MYT1 and MYT3 individually in primary human donor islets because they, but not MYT2, were regulated by nutrient signals (21). The secondary goal is to examine if these TFs regulate other T2D-risk genes.

Methods

Human donor islet procurement and mouse usage

De-identified human islets were from IIDP. After receiving, a few islets were stained with dithizone to verify islet purity, a few with DAPI to examine viability, and a few others for testing glucose responsiveness. Only islets with >90% purity, >90% viability, and stimulation index [insulin secretion at 11 mM glucose (G11)/secretion at G2.8 within a 45-min window] above 2.0 were used. Mouse usage followed the procedures approved by the Vanderbilt IACUC for Dr. Gu. Mice were housed in an SPF barrier facility in isolated standard mouse cages with free access to water and food.

Pseudo-islets preparation for gene knockdown

Lentiviral production and usage followed the routine protocol, with each expressing a control or one targeting shRNA for MYT1 or MYT3 (Fig. S1A-G). Pseudo-islet (PSI) production followed a published protocol (28). Briefly, primary human donor islets were dissociated into single cells, mixed with lentivirus, and plated into Aggrewells (96-well late, Nacali #4860-900SP) for PSI production. The media contained 50% CMRL1066 + 50% Vasculife Basal Media, 10% heat-inactivated FBS, 1X antibiotics, 0.5X Glutamax, 2.5 mM HEPES, 0.5X sodium pyruvate plus rh VEGF LifeFactor, rh EGF LifeFactor, rh FGF basic LifeFactor, rh IGF-1 LifeFactor, Ascorbic Acid LifeFactor, Hydrocortisone Hemisuccinate LifeFactor, Heparin Sulfate LifeFactor, Gentamicin/Amphotericin, L-glutamine LifeFactor B, and iCell Endothelial Cells Medium Supplement. PSIs were collected 5 days later for downstream analysis.

Immunofluorescence (IF) staining

IF staining used frozen or paraffin sections. TUNEL assay kits (Invitrogen) were used to monitor cell death. Antibodies and dilution used were: rabbit anti-Pdx1 (1:5000) and guinea pig anti-Pdx1 (1:2000) (gifts from Chris Wright, Vanderbilt University); mouse anti-glucagon (1:5000) (Dako); goat anti-somatostatin (1:500) (Millipore); rabbit anti-somatostatin (1:2000) (Santa Cruz); rabbit anti-PPY (1:500) (Abcam); guinea pig anti-insulin (1:1000) (Dako); rabbit anti-Myt1 (1:1000) (this lab); rat anti-Myt3 (1:1000) (this lab); rabbit anti-MafA (Novus, RRID: AB_1503594); and chicken anti-Nkx6.1 (Developmental Studies Hybridoma Bank, F55A10). All secondary antibodies were from Jackson ImmunoResearch, with Cat# available if requested. For imaging, slides were counter-stained with DAPI (when indicated) and imaged with laser scanning confocal microscopy (FV1000). Image J was used for quantification. All antibodies were validated with null mutants or non-expressing tissues.

Gene expression assays

Real-time qPCR used total RNA isolated with a DNA-free RNA™ kit (Zymo Research), a cDNA synthesis with a high-capacity kit (Promega), and the SYBR green master mix of the Bio-Rad system. Oligos used were: plasmid DNA: 5'-aactttggcattgtggaagg-3'+ 5'-ggatgcagggatgatgttct-3'; mCherry: 5'-aactttggcattgtggaagg-3'+ 5'-ggatgcagggatgatgttct-3; GAPDH: 5'-ctttggtatcgtggaaggactc-3' and 5'-agtagaggcagggatgatgt-3'; MYT1: 5'-ggccacatcaccgggaacta-3' and 5'-agtgggcagccatgaggttt-3'; and MYT3: 5'-ggcatgcagactctgtggct-3' and 5'-catccacagccagccattcg-3'.

Bulk RNAseq used Novaseq 6000 following the manufacturer's protocol [~120 million reads per sample]. Data analyses used the workflow in Genialis (29). Genes with TPM (transcripts per million) $\geq$ 0.5 were considered expressed, with above one RNA molecule in each cell, assuming each contains ~20 picograms of RNA (30). This identified 23,756 genes expressed in all PSIs examined (deposited in GEO). Paired t-tests were then used to identify DEGs. We consider p $\leq$0.05 with a mean difference $\geq$ 20% significant. Database for Annotation, Visualization and Integrated Discovery (DAVID) was used for functional clustering of DEGs (31). Pathways with p-values <0.05 were considered significant.

scRNA-seq used the InDrop system and Novaseq 6000 (~120 million reads per sample). DropEst was then used to preprocess scRNA-seq reads and to generate count matrices. Cells with low unique mapping reads (<500), low proportion of expressed genes (<100), or high proportion of mitochondrial RNAs (>10%) will be excluded. Reads were normalized using UMI-filtered counts. Cell subpopulations were identified and visualized by UMAP using Seurat based on the first 30 principal components generated from the top 2000 highly variable genes (32,33). DEGs between mutant and control β-cells were identified by Seurat at the criteria of |log2 fold change|> 0.25 & FDR< 0.05. Pathway analysis followed that above using DAVID.

Overlapping MYT-regulated genes with T2D-risk genes

We examined genes that are expressed in 1) human islets and 2) human β-cells separately. We used the 23,756 genes in PSIs identified above as background for human islet-related genes. For β cells, we combined the β-cell-specific genes expressed in fetal or adult β-cells at TPM>0.5 in (34) and the extra genes identified via scRNA-seq by Walker et al. (35) or us, yielding 18,743

genes. For T2D-associated genes, three lists were used: 1) All T2D-associated genes from the GWAS catalog with $p<9X10^{-6}$ (36). 2) T2D-associated genes with higher stringency ($p<5 X 10^{-8}$) in (1). 3) The DEGs between healthy and T2D donor islets (35). Each of these three lists was then used to derive two, with those associated with total islet or β-cell genes. Hypergeometric tests were used to examine the overlap.

PSI transplantation and follow-up analysis, insulin tolerance tests

PSIs transplantation into the anterior eye chambers and characterization in healthy NSG-DTR mice followed established protocols (37). The recipient mice used were 2-5 months old, with both males and females used. Mice with infection or signs of stress were euthanized without used in further experimentation. Some transplants were recovered 4 weeks after transplantation (~10am-noon) for characterization. Others were recovered and studied after 3-month HFD feeding [~60% calories from fat, Fisher Scientific (14-726-510), compared to ~13% from fat in the control diet (Lab Diet, 5001)] starting 4 weeks after transplantation. Mice were fasted for 4 hours (starting at ~8 am) for insulin tolerance tests. Insulin Humalog was injected at 0.5 Units/kg, followed by blood glucose assays at 0, 15, 30, 45, and 60 min after injection.

Hormone secretion

Insulin/glucagon secretion was stimulated with 2.8 mM glucose (G2.8) or G16.7 for 45 minutes in a standard KRB solution. The % of total hormone secreted was presented. ELISA kits from Alpco or Mercodia were used to assay insulin or glucagon, respectively.

Statistical analysis

The students' *t*-test was used to make pairwise comparisons at single time points or paired genotypes. Two-way ANOVA was used to compare multiple groups of data points. A *p*-value ≤ 0.05 was considered significant.

Data Accessibility and request for materials

The RNAseq data are deposited in the Gene Expression Omnibus (GEO) database. Resource/reagent requests will be fulfilled by the Lead Contact Guoqiang.gu@vanderbilt.edu.

Results

Knockdown of *MYT3* but not *MYT1* impaired human β-cell glucose-stimulated insulin secretion

We used shRNA-based knockdown (KD) to explore the causal relations between the reduced *MYT* expression and β-cell dysfunction. This was made possible by identifying shRNAs that could effectively target the *MYT1* or *MYT3* mRNAs in HEK293 cells (Fig. S1).

When introduced into PSIs from human primary islet cells using a lentivirus vector, these shRNAs resulted in 70-80% MYT1 or MYT3-KD, respectively, compared with controls (Fig. 1A-D). MYT3-KD, but not MYT1-KD, compromised the glucose-stimulated insulin secretion (GSIS) of PSIs compared with controls (Fig. 1E). MYT1-KD or MYT3-KD had no effect on glucagon secretion (Fig. 1F). We therefore decided to focus on β-cells.

We did not observe a significant number of cells that co-expressed insulin with glucagon, somatostatin (SST) (Fig. 1G-I), or pancreatic polypeptide (PPY) (Fig. S2A-C). Neither did we observe a significantly changed expression of representative β-cell markers such as PDX1, MAFA, and NKX6.1 (Fig. S2D-F). These findings suggest that high MYT1 or MYT3 activity is dispensable for maintaining the identity of human β-cells.

MYT1-KD but not MYT3-KD induces human β-cell death in PSIs *in vitro*

We examined whether MYT1- or MYT3-KD induced primary β-cell death. Freshly prepared PSIs were stained briefly with nuclear dye DAPI, expecting to label the nuclei of only dead cells. MYT1-KD but not MYT3-KD PSIs contained significant $DAPI^+$ cells (Fig. 2A-C). TUNEL assays showed that the insulin-expressing cells in the MYT1-KD PSIs had fragmented DNA, suggesting the apoptotic death of β-cells (Fig. 2D, E).

Because human β-cell death detected *in vitro* was sometimes not shown *in vivo* (38), we examined how β-cells with MYT1- or MYT3-KD behaved *in vivo.* PSIs were transplanted into the anterior eye chambers (AECs) of NSG-DTR mice. The transplants were recovered four weeks later for cell death assays (Fig. 2F-H). In all three donor samples tested, we found significantly more β-cell death upon MYT1-KD but not upon MYT3-KD compared with controls (Fig. 2I). These results suggest that MYT1 but not MYT3 is required for human β-cell survival under normal physiological conditions.

MYT3-KD renders human β-cells vulnerable to obesity-induced death

We then examined if MYT1- or MYT3-KD human cells are vulnerable to obesity-induced stress. Mice transplanted with control, MYT1-KD, or MYT3-KD PSIs were fed with a high-fat diet (HFD) for 12 weeks, starting 4 weeks after transplantation. This did not change fasting blood glucose levels but induced significant insulin resistance (Fig. 3A). The transplants were then recovered and assayed for β-cell death. At this recovery time, very few β-cells were left for detection in MYT1-KD samples, although many β-cells were found in control transplants (Fig. 3B, C). This is consistent with the death of most MYT1-KD β-cells but makes it a challenge for quantification (Fig. 3C). We, therefore, focused on examining the β-cells with MYT3-KD.

More β-cell death was detected in transplants with MYT3-KD than controls (Fig. 3D, E). We did not detect significant numbers of insulin+ cells co-expressing other hormones, including glucagon, SST, and PPY (Fig. 3F-K). These results suggest that MYT3-KD in human β-cells did not induce spurious activation of other islet hormones, a feature of β-cell transdifferentiation.

These combined findings suggest that MYT1 and MYT3 have overlapping but different functions in human βcells. Under normal physiology, the former is primarily required to protect cell viability, while the latter is required for secretory function. Yet, at high stress levels, both are needed for βcell viability. We next examined the gene expression changes induced by the KD of these factors.

MYT1 and MYT3 regulate common and unique gene networks in PSIs

We utilized RNAseq to examine the effect of MYT1- or MYT3-KD on gene expression in fresh PSIs, which we envision to capture the gene expression changes before cells experience physiological stress. Bulk RNAseq from intact PSIs and scRNA-seq from dissociated PSI cells were performed. The former was expected to capture MYT TF-regulated genes in all islet cells, while the latter would allow focused studies of β-cells.

Bulk RNAseq from four donor islet batches identified 23,756 genes with detectable read (methods), amongst which 2,666 or 1,099 differentially expressed genes (DEGs) between control and MYTY1-KD or MYT3-KD PSIs, respectively, were found (Fig. 4A) (Table S1, S2). Consistent with their overlapping functions, MYT1-KD and MYT3-KD share 471 DEGs (Table S2), a 1.79-fold enrichment over random gene overlap (Fig. 4B) (p=1.21E-18, hypergeometric test). We found several stress response-related genes were dysregulated with MYT1- or MYT3-KD or both conditions (Fig. 4C), consistent with the known roles of Myt TFs in stress response. These include activating TFs genes (e.g., *ATF7, HSF4*) that are involved in stress response (39,40), *ATG* genes (e.g., *ATG4D, ATG7, ATG9A, ATG10*) that are involved in autophagy (41), two families of heat shock-proteins (*DNAJB5, DNAJC13, DNAJC3, DNAJC27, HSPA2,* and *HSPD1*) involved in

cytoplasmic unfolded stress response, and a few other detoxicating enzymes (*DERL3, CAT*) (Fig. 4C) (21). Note that we only detected significant down-regulation of MYT1 or MYT3 when their respective shRNA was used, verifying their specificity (Fig. 4C). No MYT1L up-regulation was detected either (Fig.4C), which could otherwise compensate the effects of MYT-KD.

Besides the above genes, we identified several DEGs that are associated with cell death and vesicular biosynthesis/secretion (Fig. 4D). Notably, cell death regulators *CASP3, Casp9* (42), and *PSMD7* (43) were upregulated in MYT1-KD PSIs but down-regulated (or not changed) in MYT3-KD samples (Fig. 4D). The expression of genes that regulate secretion, including *GLP1R* (44), *KIF3B* (45), *NSF* (46), *PCBP2* (47), and *SYT11* (48), were upregulated in the MYT1-KD but not MYT3-KD cells (Fig. 4D). These specific gene expression changes correlate with the detected cell death or dysfunction in the MYT1- or MYT3-KD cells, respectively.

Next, we examined the up-regulated or down-regulated processes in the MYT1-KD or MYT3-KD PSIs. The down-regulated pathways in MYT1-KD samples include those controlling *cell cycle, membrane, kinesin motor, MAP kinase signaling, etc.* (Fig. 4E), while up-regulated pathways include *mitochondrion, membrane, kinase, glycolysis,* Ca^{2+} *transport,* etc. (Fig. 4F). In contrast, MYT3-KD down-regulated genes mainly regulate *Golgi, G proteins,* and *Ubl conjugation pathway* but upregulate those involved in *Sulfatase-CS*, *membrane*, *repressor, cholesterol metabolism,* etc. (Fig. 4G, H).

ScRNA-seq revealed DEGs upon MYT1- or MYT3-KD specifically in β-cell

High-quality sequencing data were obtained from one batch of PSIs (Fig. S3). These contained all the major islet cell types (α, β, δ, and γ) (Fig. 5A), including 536, 906, and 661 β-cells

in control, MYT1-KD, and MYT3-KD samples, respectively. There was a clear separation of control and MYT3-KD β-cells but not between control and MYT1-KD β-cells (Fig. 5B). Accordingly, we found 687 DEGs between the control and MYT1-KD samples and 3,284 DEGs between the control and MYT3-KD samples (Fig. 5C) (Table S3, S4). Consistent with successful KD, there was a significant reduction of *MYT3* transcripts in the MYT3-KD samples (Table S4). The lack of separation between control and MYT1-KD cells and the lower number of DEGs between control and MYT1-KD β-cells likely resulted from the death of the β-cells with high levels of MYT1-KD. In addition, we found 530 DEGs shared between those deregulated by MYT1-KD or MYT3-KD, a 5.23-fold enrichment over random overlap between β-cell-expressed genes (p=1.48E-420, hypergeometric tests) (Fig. 5D) (Table S4). These latter findings underscore the similar functions of these TFs in human β-cells.

We examined the pathways affected by MYT1- or MYT3-KD in β-cells. MYT1-KD upregulated two main processes, *cytosolic ribosome* and *Ubl conjugation* (Fig. 5E), while down-regulating processes such as *ATP binding*, *Ca^{2+} binding,* and synapse-related processes (Fig. 5F). In contrast, MYT3-KD upregulated processes such as *mitochondrial membrane, microtubule, ER to Golgi trafficking, SNARE binding, K^+ channels,* etc. (Fig. 5G). MYT3-KD also down-regulates processes such as *Ubl conjugation, protein kinases, overall transcription, microtubule*, etc. (Fig. 5H). These processes may contribute to β-cell function by mediating stress responses (via, e.g., the Ubl-related process), Ca^{2+} handling (via channel activities), and secretion (microtubule mediated transport, Ca^{2+} influx). Notably, these β-cell specific pathways also differ from those of the entire cell populations from PSIs, suggesting that the MYT TFs may regulate different processes in different cell types.

Human MYT1- and MYT3-regulated genes are enriched for T2D-associated genes

Because all three MYT gene family members are associated with T2D risk, we examined whether deregulated genes in MYT1- of MYT3-KD samples are enriched for those associated with higher T2D risk. We obtained several data sets: 1) all T2D-risk genes in GWAS Catalog, including 2,169 genes (GWAS-list) (36), from which we established 1,593 human islet- or 1,347 β-cell-expressed gene sets (Table S5, S6); 2) the recently-published T2D-associated genes with a more stringent cutoff of p<5E-10 (Suzuki-list) from which we established a 622 human islet- and 623 β-cell-expressed gene sets (Table S7, S8) (1); and 3) the DEGs (Walker-list) in the islets (709) (Table S9) or β-cells (365) (Table S10) of control and T2D human donors (35). We used the 18,743 genes detected in β-cells for overlapping analysis as background (methods).

Comparing the genes expressed in islets first, we found 391, 157, and 171 DEGs caused by MYT1-KD, and 132, 53, and 67 DEGs caused by MYT3-KD were found in the GWAS list, Suzuki list, or Walker list, respectively, all representing significant enrichment ($p \leq 0.01$, hypergeometric test) (Fig. 6A-C). Using a similar approach, we found that the β-cell-expressed GWAS-list, Suzuki-list, or Walker-list shares 116, 55, and 18 genes with DEGs caused by MYT1-KD, and 448, 223, and 84 genes with those caused MYT3-KD (Fig. 6D-F). All these overlaps, except the one between Walker-list and DEGs in MYT1-KD (Fig. 6F), represent significant enrichments ($p \leq 0.004$, hypergeometric test).

We last examined whether genes shared by T2D-risk, MYT1-KD, and MYT3-KD were enriched for specific processes. Four processes were found enriched ($p<0.05$) in the 45 overlapped genes amongst the Suzuki-β list and MYT-KD DEG genes, *Brain Development,*

Chromatin regulator, positive regulation of transcription by RNA pol II, and plasma membrane (Fig. 6G). Two processes were enriched in the 96 overlapped genes amongst the GWAS-β list and MYT-KD DEGs, *Chromatin regulator* and *Neurogenesis* (Fig. 6H). These results are consistent with the involvement of MYT TFs in neuronal development/function that overlaps with islet development/function and the weak contribution of each genetic mutation to human T2D.

Discussion

The interactions between genetic predisposition and metabolic load induce β-cell failure, a direct cause of T2D. Yet the mechanisms underlying these interactions remain poorly understood. Findings here, with our previous results (21), suggest that the MYT TFs constitute a key regulatory node of several T2D risk genes to prevent β-cell failure in response to nutritional signals.

Several lines of evidence support the roles of MYT TFs in human β-cells and T2D. Glucose and free fatty acids regulate the protein abundance and/or nuclear localization of MYT1 and MYT3 in primary human β-cells (21). All three genes are associated with human T2D (36). There is an anti-correlation between MYT TF levels and human β-cell function during T2D development (21). The co-KD of the three TFs in a human β-cell line induced cell death (21). Now, we directly show that MYT1-KD did not impact β-cell GSIS but led to β-cell apoptosis under normal physiology. In contrast, MYT3-KD compromised GSIS but did not impact cell viability under normal physiology. Intriguingly, MYT3-KD predisposed human β-cells to obesity-induced death as xenotransplants. Corresponding to their similar yet different biological functions, we found that MYT1 and MYT3 regulated common and unique sets of genes in islets and β-cells. More importantly, both MYT1 or MYT3-KD deregulated genes are enriched for those associated with T2D risk.

Our new findings have several implications. First, the MYT TFs may constitute a nutrient-responsive hub that integrates both genetic and environmental factors to prevent β-cell failure. To this end, high glucose or high free fatty acids, usually associated with obesity, are known to cause the overproduction of unfolded proteins or reactive oxygen species in β-cells (7). For homeostasis, β-cells activate stress response for their removal. Yet sustained or over-activation

of the stress response can also lead to β-cell failure by overly reducing essential β-cell factors or inducing cell death. In mice, the Myt TFs act as safeguards for this latter scenario because they directly prevent the overactivation of several stress response genes while maintaining the expression of several other essential β-cell genes (21). We now demonstrate that this MYT-dependent β-cell protection can be extended to human primary β-cells via several T2D-risk genes. These findings, together with the nutrient-regulatability of the MYT TFs in human β-cells (21), suggest the key roles of these TFs in mediating the combined effects of genetic and nutritional signals on β-cell failure. Second, despite the high similarity between MYT1 and MYT3 proteins (49,50), they complement each other to prevent β-cell failure under various physiological stresses. Specifically, MYT1 appears to have more critical roles for β-cell survival compared with MYT3, while MYT3 is more important for secretory function. This could be a reason why the expression of both is necessary for normal β-cell maintenance. Third, our findings highlight the species-specific roles of these factors in β-cells. Unlike in human cells, *Myt1* inactivation in mouse islets caused β-cell dysfunction but did not affect β-cell survival (22). Similarly, although both MYT3-KD in human β-cells and *Myt3-KO* in mouse β-cells reduced β-cell GSIS but not cell viability under normal physiology (Hu and Gu, in preparation), the MYT3-KD-predisposed human β-cell death was not detected in *Myt3-KO* mouse cells (Hu and Gu, in preparation). In addition, although multi-hormone expressing islet cells were observed in *Myt1*-single and *Myt TF*-triple mutant mouse β-cells, a property of transdifferentiating cells, they were not induced by MYT1- or MYT3-KD in primary human islet cells.

There are several issues that we have not addressed in these studies. First, although the gene KD setting is more likely to reflect the MYT activity reduction during T2D development (21),

it is unclear if such models (with <85% reduction) can reveal the full extent of molecular changes by complete loss of MYT1/MYT3. Second, due to the scarcity of human donor islets, we have not tested how the co-presence of high glucose and free fatty acids impacts the manipulated β-cells. Third, for a similar reason as above, we have not tested the effect of MYT2-KD in primary human β-cells. Thus, it is unclear whether its activity may be differentially affected by the lack of MYT1 or MYT3 to contribute to the differentially observed phenotypes. Lastly, because of β-cell death induced by high levels of MYT1-KD but not MYT3-KD, we may have missed several MYT1-regulated genes in β-cells that are essential for β-cell survival. This complication could have contributed to the higher number of DEGs in MYT1-KD PSIs (including large portions of non-β-cells) than MYT3-KD PSIs but the lower number of DEGs in MYT1-KD compared with MYT3-KD β-cells.

Acknowledgment

Author contributions

RH, MY, XT, and GG performed human islet picking, PSI production, GSIS, IF assays, and imaging. RH performed ITT, and TD performed PSI transplantation. JL helped with viral production and PSI growth. YW and QL analyzed scRNA-seq data. NH did T2D association studies, and YX, AJS, and KSL performed scRNA-seq using InDrop. RS, IK, QL, KC, and GG conceptualized the study. All authors participated in manuscript writing/proofing.

Funding

This study is supported by NIH grants (DK125696 and DK128710 for GG, DK103831, and CA095103 for KSL, YX, and AJS. The imaging facility used is funded by (CA68485, DK20593, DK58404, DK59637, and EY08126).

References cited

1. Suzuki K, Hatzikotoulas K, Southam L, Taylor HJ, Yin X, Lorenz KM, Mandla R, Huerta-Chagoya A, Melloni GEM, Kanoni S, Rayner NW, Bocher O, Arruda AL, Sonehara K, Namba S, Lee SSK, Preuss MH, Petty LE, Schroeder P, Vanderwerff B, Kals M, Bragg F, Lin K, Guo X, Zhang W, Yao J, Kim YJ, Graff M, Takeuchi F, Nano J, Lamri A, Nakatochi M, Moon S, Scott RA, Cook JP, Lee JJ, Pan I, Taliun D, Parra EJ, Chai JF, Bielak LF, Tabara Y, Hai Y, Thorleifsson G, Grarup N, Sofer T, Wuttke M, Sarnowski C, Gieger C, Nousome D, Trompet S, Kwak SH, Long J, Sun M, Tong L, Chen WM, Nongmaithem SS, Noordam R, Lim VJY, Tam CHT, Joo YY, Chen CH, Raffield LM, Prins BP, Nicolas A, Yanek LR, Chen G, Brody JA, Kabagambe E, An P, Xiang AH, Choi HS, Cade BE, Tan J, Broadaway KA, Williamson A, Kamali Z, Cui J, Thangam M, Adair LS, Adeyemo A, Aguilar-Salinas CA, Ahluwalia TS, Anand SS, Bertoni A, Bork-Jensen J, Brandslund I, Buchanan TA, Burant CF, Butterworth AS, Canouil M, Chan JCN, Chang LC, Chee ML, Chen J, Chen SH, Chen YT, Chen Z, Chuang LM, Cushman M, Danesh J, Das SK, de Silva HJ, Dedoussis G, Dimitrov L, Doumatey AP, Du S, Duan Q, Eckardt KU, Emery LS, Evans DS, Evans MK, Fischer K, Floyd JS, Ford I, Franco OH, Frayling TM, Freedman BI, Genter P, Gerstein HC, Giedraitis V, Gonzalez-Villalpando C, Gonzalez-Villalpando ME, Gordon-Larsen P, Gross M, Guare LA, Hackinger S, Hakaste L, Han S, Hattersley AT, Herder C, Horikoshi M, Howard AG, Hsueh W, Huang M, Huang W, Hung YJ, Hwang MY, Hwu CM, Ichihara S, Ikram MA, Ingelsson M, Islam MT, Isono M, Jang HM, Jasmine F, Jiang G, Jonas JB, Jorgensen T, Kamanu FK, Kandeel FR, Kasturiratne A, Katsuya T, Kaur V, Kawaguchi T, Keaton JM, Kho AN, Khor CC, Kibriya MG, Kim DH, Kronenberg F, Kuusisto J, Lall K, Lange LA, Lee KM, Lee MS, Lee NR, Leong A, Li L, Li Y, Li-Gao R, Ligthart S, Lindgren CM, Linneberg A, Liu CT, Liu J, Locke AE, Louie T, Luan J, Luk AO, Luo X, Lv J, Lynch JA, Lyssenko V, Maeda S, Mamakou V, Mansuri SR, Matsuda K, Meitinger T, Melander O, Metspalu A, Mo H, Morris AD, Moura FA, Nadler JL, Nalls MA, Nayak U, Ntalla I, Okada Y, Orozco L, Patel SR, Patil S, Pei P, Pereira MA, Peters A, Pirie FJ, Polikowsky HG, Porneala B, Prasad G, Rasmussen-Torvik LJ, Reiner AP, Roden M, Rohde R, Roll K, Sabanayagam C, Sandow K, Sankareswaran A, Sattar N, Schonherr S, Shahriar M, Shen B, Shi J, Shin DM, Shojima N, Smith JA, So WY, Stancakova A, Steinthorsdottir V, Stilp AM, Strauch K, Taylor KD, Thorand B, Thorsteinsdottir U, Tomlinson B, Tran TC, Tsai FJ, Tuomilehto J, Tusie-Luna T, Udler MS, Valladares-Salgado A, van Dam RM, van Klinken JB, Varma R, Wacher-Rodarte N, Wheeler E, Wickremasinghe AR, van Dijk KW, Witte DR, Yajnik CS, Yamamoto K, Yamamoto K, Yoon K, Yu C, Yuan JM, Yusuf S, Zawistowski M, Zhang L, Zheng W, Program VAMV, Raffel LJ, Igase M, Ipp E, Redline S, Cho YS, Lind L, Province MA, Fornage M, Hanis CL, Ingelsson E, Zonderman AB, Psaty BM, Wang YX, Rotimi CN, Becker DM, Matsuda F, Liu Y, Yokota M, Kardia SLR, Peyser PA, Pankow JS, Engert JC, Bonnefond A, Froguel P, Wilson JG, Sheu WHH, Wu JY, Hayes MG, Ma RCW, Wong TY, Mook-Kanamori DO, Tuomi T, Chandak GR, Collins FS, Bharadwaj D, Pare G, Sale MM, Ahsan H, Motala AA, Shu XO, Park KS, Jukema JW, Cruz M, Chen YI, Rich SS, McKean-Cowdin R, Grallert H, Cheng CY, Ghanbari M, Tai ES, Dupuis J, Kato N, Laakso M, Kottgen A, Koh WP, Bowden DW, Palmer CNA, Kooner JS, Kooperberg C, Liu S, North KE, Saleheen D, Hansen T, Pedersen O, Wareham NJ, Lee J, Kim BJ, Millwood IY, Walters RG, Stefansson K, Ahlqvist

E, Goodarzi MO, Mohlke KL, Langenberg C, Haiman CA, Loos RJF, Florez JC, Rader DJ, Ritchie MD, Zollner S, Magi R, Marston NA, Ruff CT, van Heel DA, Finer S, Denny JC, Yamauchi T, Kadowaki T, Chambers JC, Ng MCY, Sim X, Below JE, Tsao PS, Chang KM, McCarthy MI, Meigs JB, Mahajan A, Spracklen CN, Mercader JM, Boehnke M, Rotter JI, Vujkovic M, Voight BF, Morris AP, Zeggini E. Genetic drivers of heterogeneity in type 2 diabetes pathophysiology. *Nature*. 2024;627(8003):347-357.

2. Xue D, Narisu N, Taylor DL, Zhang M, Grenko C, Taylor HJ, Yan T, Tang X, Sinha N, Zhu J, Vandana JJ, Nok Chong AC, Lee A, Mansell EC, Swift AJ, Erdos MR, Zhong A, Bonnycastle LL, Zhou T, Chen S, Collins FS. Functional interrogation of twenty type 2 diabetes-associated genes using isogenic human embryonic stem cell-derived beta-like cells. *Cell Metab*. 2023;35(11):1897-1914 e1811.
3. Marselli L, Piron A, Suleiman M, Colli ML, Yi X, Khamis A, Carrat GR, Rutter GA, Bugliani M, Giusti L, Ronci M, Ibberson M, Turatsinze JV, Boggi U, De Simone P, De Tata V, Lopes M, Nasteska D, De Luca C, Tesi M, Bosi E, Singh P, Campani D, Schulte AM, Solimena M, Hecht P, Rady B, Bakaj I, Pocai A, Norquay L, Thorens B, Canouil M, Froguel P, Eizirik DL, Cnop M, Marchetti P. Persistent or Transient Human beta Cell Dysfunction Induced by Metabolic Stress: Specific Signatures and Shared Gene Expression with Type 2 Diabetes. *Cell Rep*. 2020;33(9):108466.
4. Sharma RB, Landa-Galvan HV, Alonso LC. Living Dangerously: Protective and Harmful ER Stress Responses in Pancreatic beta-Cells. *Diabetes*. 2021;70(11):2431-2443.
5. Shrestha N, De Franco E, Arvan P, Cnop M. Pathological beta-Cell Endoplasmic Reticulum Stress in Type 2 Diabetes: Current Evidence. *Front Endocrinol (Lausanne)*. 2021;12:650158.
6. Kaneto H, Kimura T, Shimoda M, Obata A, Sanada J, Fushimi Y, Matsuoka TA, Kaku K. Molecular Mechanism of Pancreatic beta-Cell Failure in Type 2 Diabetes Mellitus. *Biomedicines*. 2022;10(4).
7. Kulkarni A, Muralidharan C, May SC, Tersey SA, Mirmira RG. Inside the beta Cell: Molecular Stress Response Pathways in Diabetes Pathogenesis. *Endocrinology*. 2022;164(1).
8. Yong J, Johnson JD, Arvan P, Han J, Kaufman RJ. Therapeutic opportunities for pancreatic beta-cell ER stress in diabetes mellitus. *Nat Rev Endocrinol*. 2021;17(8):455-467.
9. Gonzalez P, Lozano P, Ros G, Solano F. Hyperglycemia and Oxidative Stress: An Integral, Updated and Critical Overview of Their Metabolic Interconnections. *Int J Mol Sci*. 2023;24(11).
10. Guo S, Dai C, Guo M, Taylor B, Harmon JS, Sander M, Robertson RP, Powers AC, Stein R. Inactivation of specific beta cell transcription factors in type 2 diabetes. *J Clin Invest*. 2013;123(8):3305-3316.
11. Eguchi N, Vaziri ND, Dafoe DC, Ichii H. The Role of Oxidative Stress in Pancreatic beta Cell Dysfunction in Diabetes. *Int J Mol Sci*. 2021;22(4).
12. Yong J, Parekh VS, Reilly SM, Nayak J, Chen Z, Lebeaupin C, Jang I, Zhang J, Prakash TP, Sun H, Murray S, Guo S, Ayala JE, Satin LS, Saltiel AR, Kaufman RJ. Chop/Ddit3 depletion in beta cells alleviates ER stress and corrects hepatic steatosis in mice. *Sci Transl Med*. 2021;13(604).

13. Herbert TP, Laybutt DR. A Reevaluation of the Role of the Unfolded Protein Response in Islet Dysfunction: Maladaptation or a Failure to Adapt? *Diabetes*. 2016;65(6):1472-1480.
14. Yang X, Graff SM, Heiser CN, Ho KH, Chen B, Simmons AJ, Southard-Smith AN, David G, Jacobson DA, Kaverina I, Wright CVE, Lau KS, Gu G. Coregulator Sin3a Promotes Postnatal Murine beta-Cell Fitness by Regulating Genes in Ca(2+) Homeostasis, Cell Survival, Vesicle Biosynthesis, Glucose Metabolism, and Stress Response. *Diabetes*. 2020;69(6):1219-1231.
15. Yokoyama A, Igarashi K, Sato T, Takagi K, Otsuka IM, Shishido Y, Baba T, Ito R, Kanno J, Ohkawa Y, Morohashi K, Sugawara A. Identification of myelin transcription factor 1 (MyT1) as a subunit of the neural cell type-specific lysine-specific demethylase 1 (LSD1) complex. *J Biol Chem*. 2014;289(26):18152-18162.
16. Blanchet P, Bebin M, Bruet S, Cooper GM, Thompson ML, Duban-Bedu B, Gerard B, Piton A, Suckno S, Deshpande C, Clowes V, Vogt J, Turnpenny P, Williamson MP, Alembik Y, Clinical Sequencing Exploratory Research Study C, Deciphering Developmental Disorders C, Glasgow E, McNeill A. MYT1L mutations cause intellectual disability and variable obesity by dysregulating gene expression and development of the neuroendocrine hypothalamus. *PLoS Genet*. 2017;13(8):e1006957.
17. Chen J, Sun M, Adeyemo A, Pirie F, Carstensen T, Pomilla C, Doumatey AP, Chen G, Young EH, Sandhu M, Morris AP, Barroso I, McCarthy MI, Mahajan A, Wheeler E, Rotimi CN, Motala AA. Genome-wide association study of type 2 diabetes in Africa. *Diabetologia*. 2019;62(7):1204-1211.
18. Tan Y, He Q, Chan KHK. Identification of shared genetic architecture between non-alcoholic fatty liver disease and type 2 diabetes: A genome-wide analysis. *Front Endocrinol (Lausanne)*. 2023;14:1050049.
19. Hamet P, Haloui M, Harvey F, Marois-Blanchet FC, Sylvestre MP, Tahir MR, Simon PH, Kanzki BS, Raelson J, Long C, Chalmers J, Woodward M, Marre M, Harrap S, Tremblay J. PROX1 gene CC genotype as a major determinant of early onset of type 2 diabetes in slavic study participants from Action in Diabetes and Vascular Disease: Preterax and Diamicron MR Controlled Evaluation study. *J Hypertens*. 2017;35 Suppl 1(Suppl 1):S24-S32.
20. Im C, Neupane A, Baedke JL, Lenny B, Delaney A, Dixon SB, Chow EJ, Mostoufi-Moab S, Yang T, Richard MA, Gramatges MM, Lupo PJ, Sharafeldin N, Bhatia S, Armstrong GT, Hudson MM, Ness KK, Robison LL, Yasui Y, Wilson CL, Sapkota Y. Trans-Ancestral Genetic Risk Factors for Treatment-Related Type 2 Diabetes Mellitus in Survivors of Childhood Cancer. *J Clin Oncol*. 2024;42(19):2306-2316.
21. Hu R, Walker E, Huang C, Xu Y, Weng C, Erickson GE, Coldren A, Yang X, Brissova M, Kaverina I, Balamurugan AN, Wright CVE, Li Y, Stein R, Gu G. Myt Transcription Factors Prevent Stress-Response Gene Overactivation to Enable Postnatal Pancreatic beta Cell Proliferation, Function, and Survival. *Dev Cell*. 2020;53(4):390-405 e310.
22. Wang S, Zhang J, Zhao A, Hipkens S, Magnuson MA, Gu G. Loss of Myt1 function partially compromises endocrine islet cell differentiation and pancreatic physiological function in the mouse. *Mech Dev*. 2007;124(11-12):898-910.
23. Brown M, Agan V, Nevills S, Hu R, Simmons A, Xu Y, Yang Y, Yagan M, Najam MS, Dadi P, Sampson L, Magnuson MA, Jacobson DA, Lau K, Hodges E, Gu G. Endocrine islet β-cell

subtypes with differential function are derived from biochemically distinct embryonic endocrine islet progenitors that are regulated by maternal nutrients. 2024;https://www.ncbi.nlm.nih.gov/pmc/articles/PMC10942487/.

24. Fusakio ME, Willy JA, Wang Y, Mirek ET, Al Baghdadi RJ, Adams CM, Anthony TG, Wek RC. Transcription factor ATF4 directs basal and stress-induced gene expression in the unfolded protein response and cholesterol metabolism in the liver. *Mol Biol Cell*. 2016;27(9):1536-1551.
25. Han J, Back SH, Hur J, Lin YH, Gildersleeve R, Shan J, Yuan CL, Krokowski D, Wang S, Hatzoglou M, Kilberg MS, Sartor MA, Kaufman RJ. ER-stress-induced transcriptional regulation increases protein synthesis leading to cell death. *Nat Cell Biol*. 2013;15(5):481-490.
26. Yagan MN, S.; Hu, R.; Wang, Y.; Dickerson, M., Dadi, P.; Xu, Y.; Simmons, A. J.; Stein, R.; Adams, C. M.; Jacobson, D. A.,;Lau, K.; Liu, Q.; Gu, G. . Atf4 protects islet beta-cell identity and function under acute glucose-induced stress but promotes beta-cell failure in the presence of free fatty acid. *Diabetes*. 2025;In press.
27. Quiros PM, Prado MA, Zamboni N, D'Amico D, Williams RW, Finley D, Gygi SP, Auwerx J. Multi-omics analysis identifies ATF4 as a key regulator of the mitochondrial stress response in mammals. *J Cell Biol*. 2017;216(7):2027-2045.
28. Walker JT, Haliyur R, Nelson HA, Ishahak M, Poffenberger G, Aramandla R, Reihsmann C, Luchsinger JR, Saunders DC, Wang P, Garcia-Ocana A, Bottino R, Agarwal A, Powers AC, Brissova M. Integrated human pseudoislet system and microfluidic platform demonstrate differences in GPCR signaling in islet cells. *JCI Insight*. 2020;5(10).
29. Tong X, Stein R. Lipid Droplets Protect Human beta-Cells From Lipotoxicity-Induced Stress and Cell Identity Changes. *Diabetes*. 2021;70(11):2595-2607.
30. QiaGen. How much RNA does a typical mammalian cell contain.
31. Sherman BT, Hao M, Qiu J, Jiao X, Baseler MW, Lane HC, Imamichi T, Chang W. DAVID: a web server for functional enrichment analysis and functional annotation of gene lists (2021 update). *Nucleic Acids Res*. 2022;50(W1):W216-W221.
32. Butler A, Hoffman P, Smibert P, Papalexi E, Satija R. Integrating single-cell transcriptomic data across different conditions, technologies, and species. *Nat Biotechnol*. 2018;36(5):411-420.
33. Stuart T, Butler A, Hoffman P, Hafemeister C, Papalexi E, Mauck WM, 3rd, Hao Y, Stoeckius M, Smibert P, Satija R. Comprehensive Integration of Single-Cell Data. *Cell*. 2019;177(7):1888-1902 e1821.
34. Blodgett DM, Nowosielska A, Afik S, Pechhold S, Cura AJ, Kennedy NJ, Kim S, Kucukural A, Davis RJ, Kent SC, Greiner DL, Garber MG, Harlan DM, diIorio P. Novel Observations From Next-Generation RNA Sequencing of Highly Purified Human Adult and Fetal Islet Cell Subsets. *Diabetes*. 2015;64(9):3172-3181.
35. Walker JT, Saunders DC, Rai V, Chen HH, Orchard P, Dai C, Pettway YD, Hopkirk AL, Reihsmann CV, Tao Y, Fan S, Shrestha S, Varshney A, Petty LE, Wright JJ, Ventresca C, Agarwala S, Aramandla R, Poffenberger G, Jenkins R, Mei S, Hart NJ, Phillips S, Kang H, Greiner DL, Shultz LD, Bottino R, Liu J, Below JE, Consortium H, Parker SCJ, Powers AC, Brissova M. Genetic risk converges on regulatory networks mediating early type 2 diabetes. *Nature*. 2023;624(7992):621-629.

36. Cerezo M, Sollis E, Ji Y, Lewis E, Abid A, Bircan KO, Hall P, Hayhurst J, John S, Mosaku A, Ramachandran S, Foreman A, Ibrahim A, McLaughlin J, Pendlington Z, Stefancsik R, Lambert SA, McMahon A, Morales J, Keane T, Inouye M, Parkinson H, Harris LW. The NHGRI-EBI GWAS Catalog: standards for reusability, sustainability and diversity. *Nucleic Acids Res*. 2025;53(D1):D998-D1005.
37. Yang C, Loehn M, Jurczyk A, Przewozniak N, Leehy L, Herrera PL, Shultz LD, Greiner DL, Harlan DM, Bortell R. Lixisenatide accelerates restoration of normoglycemia and improves human beta-cell function and survival in diabetic immunodeficient NOD-scid IL-2rg(null) RIP-DTR mice engrafted with human islets. *Diabetes Metab Syndr Obes*. 2015;8:387-398.
38. Dai C, Kayton NS, Shostak A, Poffenberger G, Cyphert HA, Aramandla R, Thompson C, Papagiannis IG, Emfinger C, Shiota M, Stafford JM, Greiner DL, Herrera PL, Shultz LD, Stein R, Powers AC. Stress-impaired transcription factor expression and insulin secretion in transplanted human islets. *J Clin Invest*. 2016;126(5):1857-1870.
39. Takii R, Fujimoto M, Tan K, Takaki E, Hayashida N, Nakato R, Shirahige K, Nakai A. ATF1 modulates the heat shock response by regulating the stress-inducible heat shock factor 1 transcription complex. *Mol Cell Biol*. 2015;35(1):11-25.
40. Maekawa T, Liu B, Liu Y, Yoshida K, Muratani M, Chatton B, Ishii S. Stress-induced and ATF7-dependent epigenetic change influences cellular senescence. *Genes Cells*. 2019;24(9):627-635.
41. Levine B, Kroemer G. Biological Functions of Autophagy Genes: A Disease Perspective. *Cell*. 2019;176(1-2):11-42.
42. Liadis N, Murakami K, Eweida M, Elford AR, Sheu L, Gaisano HY, Hakem R, Ohashi PS, Woo M. Caspase-3-dependent beta-cell apoptosis in the initiation of autoimmune diabetes mellitus. *Mol Cell Biol*. 2005;25(9):3620-3629.
43. Xu X, Xuan X, Zhang J, Xu H, Yang X, Zhang L, Zhao Y, Xu H, Li D. PSMD7 downregulation suppresses lung cancer progression by regulating the p53 pathway. *J Cancer*. 2021;12(16):4945-4957.
44. Cataldo LR, Vishnu N, Singh T, Bertonnier-Brouty L, Bsharat S, Luan C, Renstrom E, Prasad RB, Fex M, Mulder H, Artner I. The MafA-target gene PPP1R1A regulates GLP1R-mediated amplification of glucose-stimulated insulin secretion in beta-cells. *Metabolism*. 2021;118:154734.
45. Wang S, Tanaka Y, Xu Y, Takeda S, Hirokawa N. KIF3B promotes a PI3K signaling gradient causing changes in a Shh protein gradient and suppressing polydactyly in mice. *Dev Cell*. 2022;57(19):2273-2289 e2211.
46. Polgar J, Reed GL. A critical role for N-ethylmaleimide-sensitive fusion protein (NSF) in platelet granule secretion. *Blood*. 1999;94(4):1313-1318.
47. Haemmerle MW, Scota AV, Khosravifar M, Varney MJ, Sen S, Good AL, Yang X, Wells KL, Sussel L, Rozo AV, Doliba NM, Ghanem LR, Stoffers DA. RNA-binding protein PCBP2 regulates pancreatic beta cell function and adaptation to glucose. *J Clin Invest*. 2024;134(12).
48. Li WR, Wang YL, Li C, Gao P, Zhang FF, Hu M, Li JC, Zhang S, Li R, Zhang CX. Synaptotagmin-11 inhibits spontaneous neurotransmission through vti1a. *J Neurochem*. 2021;159(4):729-741.

49. Henry C, Close AF, Buteau J. A critical role for the neural zinc factor ST18 in pancreatic beta-cell apoptosis. *J Biol Chem*. 2014;289(12):8413-8419.
50. Yang J, Siqueira MF, Behl Y, Alikhani M, Graves DT. The transcription factor ST18 regulates proapoptotic and proinflammatory gene expression in fibroblasts. *FASEB J*. 2008;22(11):3956-3967.

Figures and legends

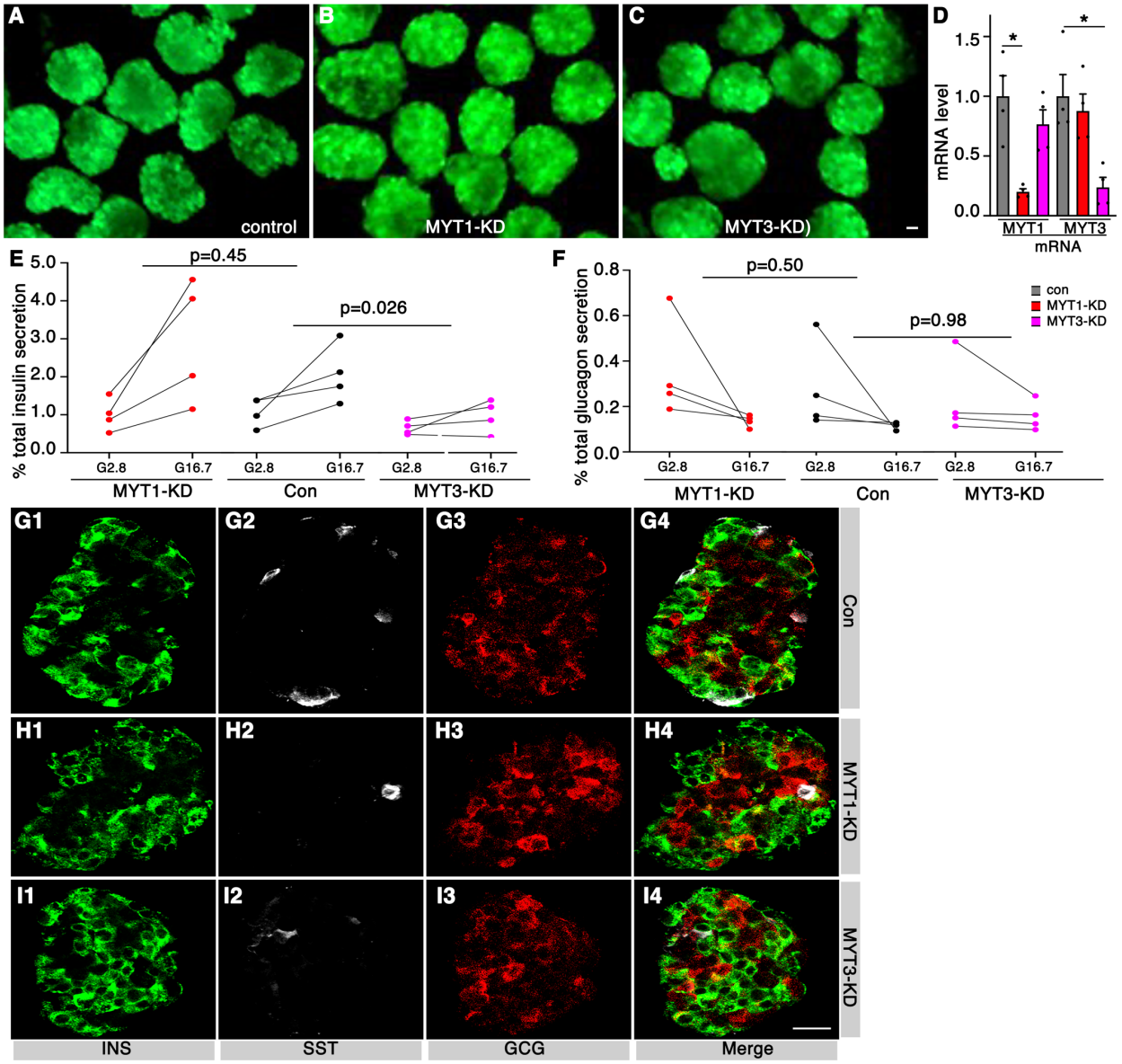

Fig. 1. MYT3-KD, but not MYT1-KD, impaired GSIS of primary human β-cells. Procured primary human islets, after quality check, were dissociated into single cells, infected with lentivirus that drives the expression of control, MYT1-targeting, or MYT3-targeting shRNAs, and made into PSIs and tested for GSIS. Islets from 4 donors were used in this study, each tested in 2-4 individual GSIS assays. (A-C) Representative PSIs, with eGFP as a marker of lentivirus infection. (D) RT-PCR assays showing MYT1- or MYT3-KD levels in one PSI batch. Shown are mean + SEM. *: $p<0.02$, calculated via t-test (with two-tailed type two errors). (E, F) Secretion assays of insulin (E) or glucagon (F) in response to G2.8 or G16.7. Each dot represents assays of one batch of PSIs, with 3 or 4 secretion assays. P values are from two-way ANOVA. (G-I) Hormone expression assays in newly-produced PSIs. Note that image panels from the same field of view were marked with the same capital letter (followed by a number to indicate different channels). Scale bars = 20 μm.

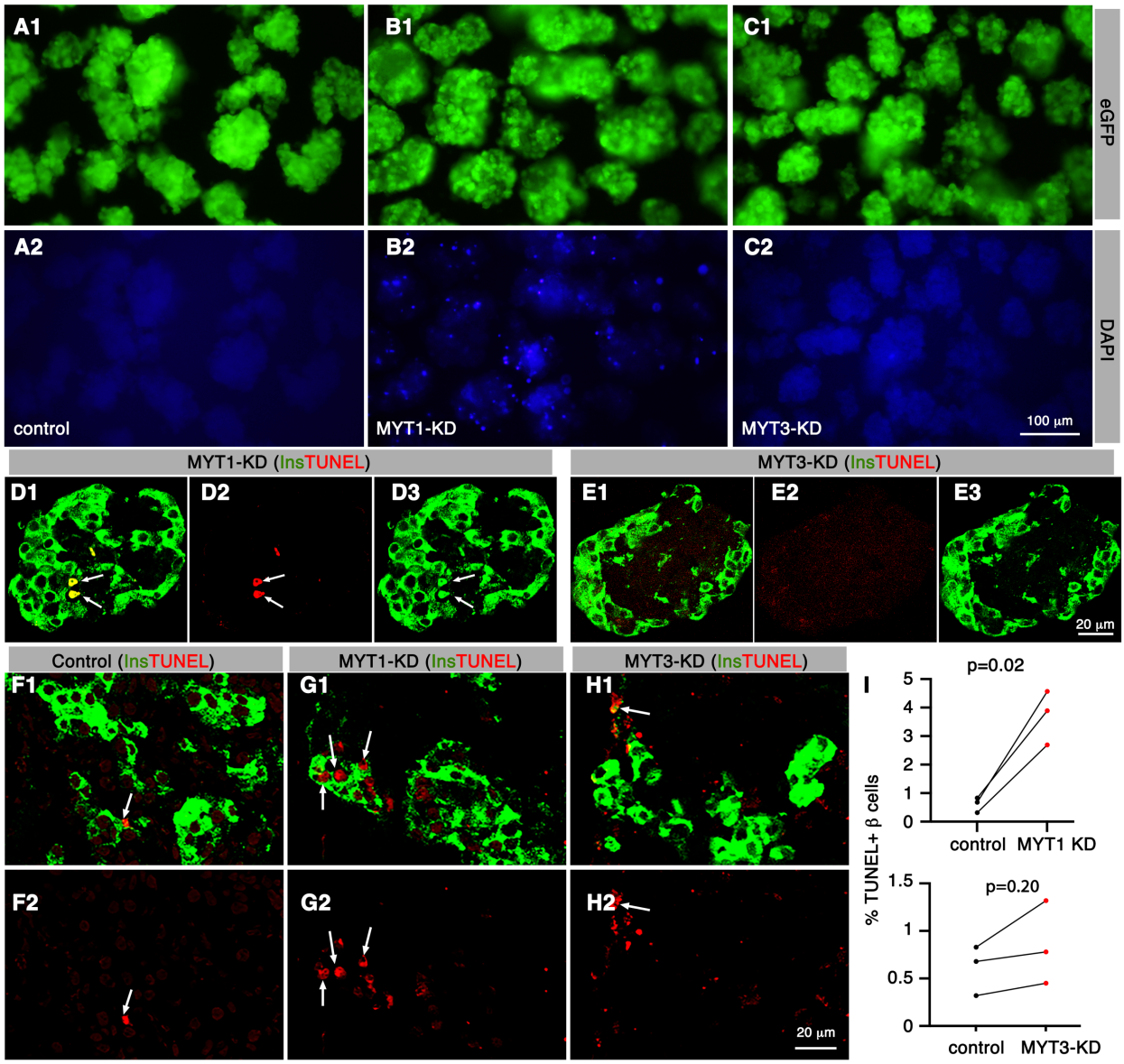

Fig. 2. MYT1-KD, but not MYT3-KD, caused the death of primary human β-cells *in vitro* and *in vivo* under normal physiology. Freshly made PSIs from four donors, with control, MYT1-KD, or MYT3-KD, were stained with DAPI to visualize dead cells. They were also examined for cell death with TUNEL assays before or 4 weeks after transplantation into the AEC of mice. (A-C) DAPI staining to show the presence of DAPI+ cells without any treatment. Note that image panels from the same field of view were marked with the same capital letter (followed by a number to indicate different channels). Also, note that panels A2 and C2 were purposely over-exposed to show the cells. (D-E) TUNEL staining of freshly made PSIs. White arrows pointed at two dead cells with Insulin-signals. (F-I) TUNEL assays and quantification of dead β-cells 4 weeks after PSIs were transplanted into AEC of mice. White arrows pointed at several dead insulin+ cells. In I, each dot represents results from one batch of islets, with each batch transplanted into at least three mice. P values were from paired t-tests (with data from the same donor pair).

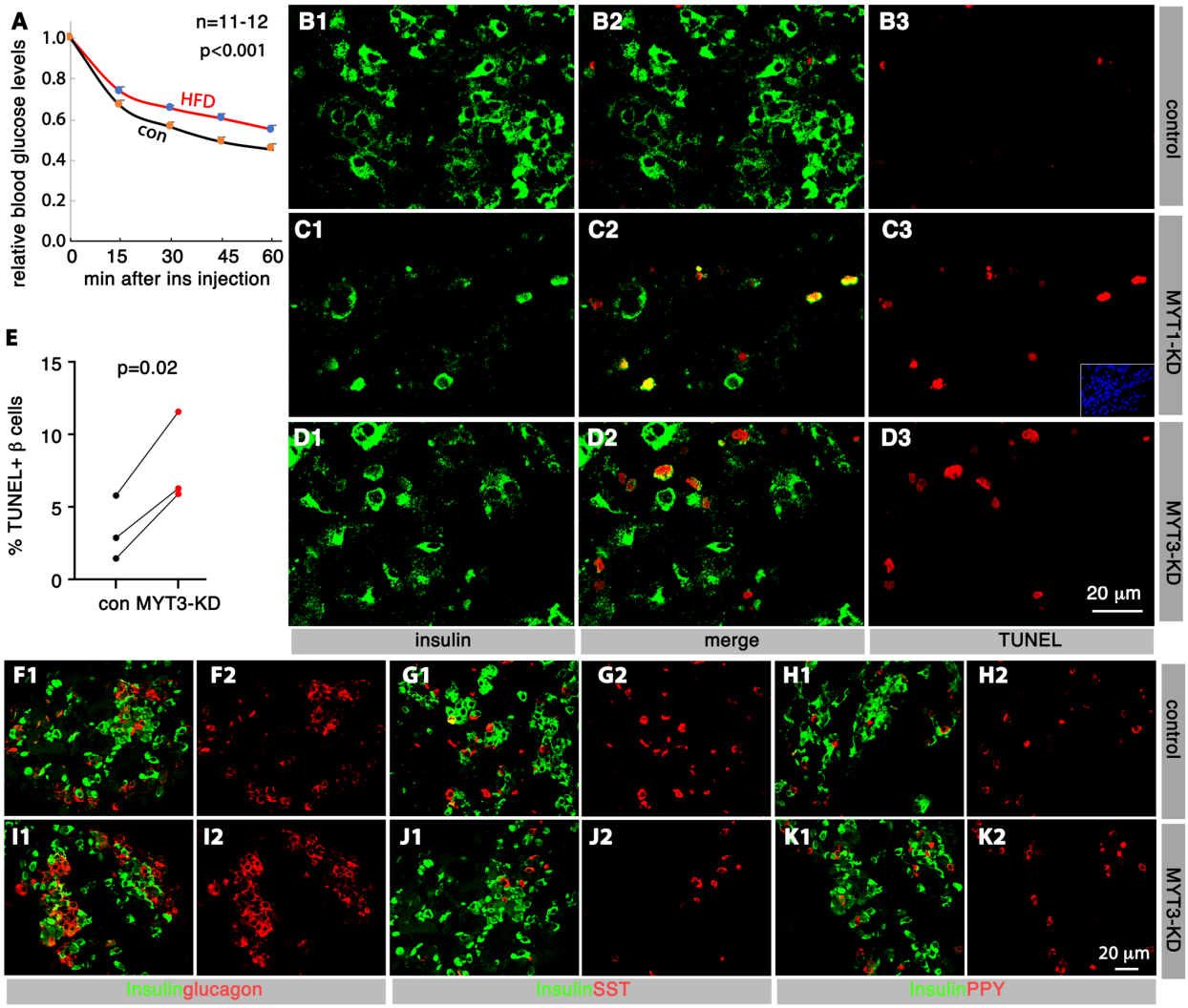

Fig. 3. MYT3-KD renders primary human β-cells vulnerable to HFD-induced cell death. Four weeks after the transplantation, mice were fed with HFD for 12 more weeks. PSIs were then recovered for characterization. PSIs from 3 donors were transplanted, each into at least three mice. (A) Insulin tolerance test to show the HFD-induced insulin resistance in recipient mice. The starting blood glucose of each animal was normalized to "1". The p-value is from two-way ANOVA. (B-E) TUNEL-assays of recovered transplants. Image panels from the same field of view were marked with the same capital letter (followed by a number to indicate different channels). Inset in C3 showed a DAPI staining in processed sections to visualize all nuclei. In E, each dot represents data from one islet batch, which included at least three transplanted mice. "P" is from paired t-tests. (F-K) IF showing the hormone co-expression status (between insulin and other hormones) in recovered transplants.

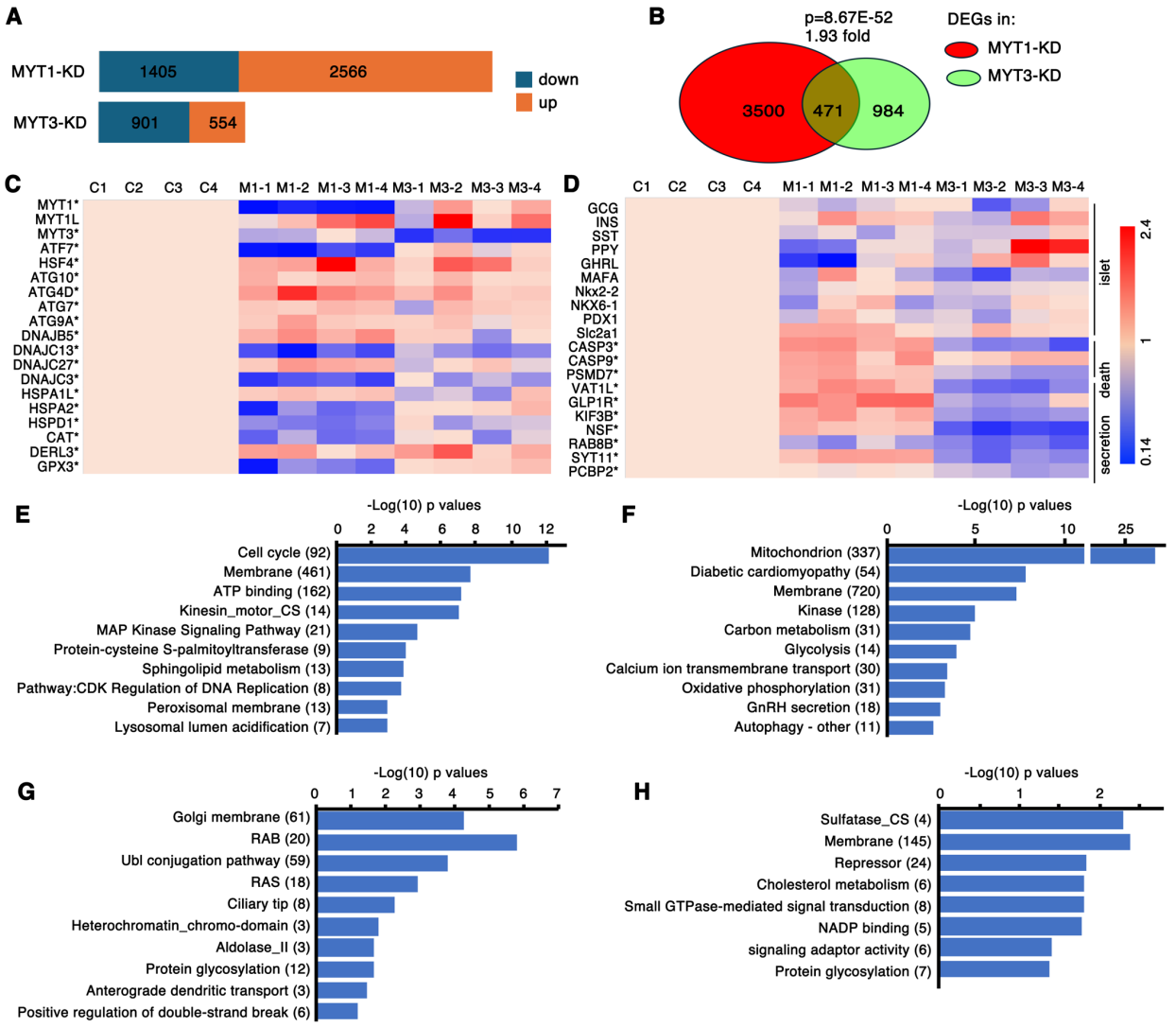

Fig. 4. Human islet cells with MYT1 or MYT3 KD deregulates overlapping but distinct genes. Freshly prepared PSIs were directly used for total RNA prep and sequencing. Four batches of donor islets were used. (A) The numbers of genes that were down- or upregulated with MYT1-KD or MYT3-KD in total PSIs. (B) The numbers of common and specific genes affected by MYT1- or MYT3-KD. (C, D) Heat maps of a few MYT1- or MYT3-regulated genes in four PSI duplicates, focusing on those involved in stress (C) or function (D). In sample annotations on the top, C1-C4 refers to the four independent controls. M1-1 to M1-4 are the four samples with MYT1-KD. M3-1 to M3-4 are the four samples with MYT3-KD. To compensate for the considerable variation of gene expression from different batches of donor islets, the gene expression levels in controls were normalized to "1". The genes marked with "*" indicate DEGs in at least one KD sample. (E, F) Pathways deregulated in MYT1-KD human PSIs, composed of down- (E) or up-regulated (F) genes in mutants. (G, H) Pathways deregulated in MYT3-KD human PSIs, composed of down- (G) or up-regulated (H) genes in mutants. The number in parenthesis following each process refers to the number of genes discovered.

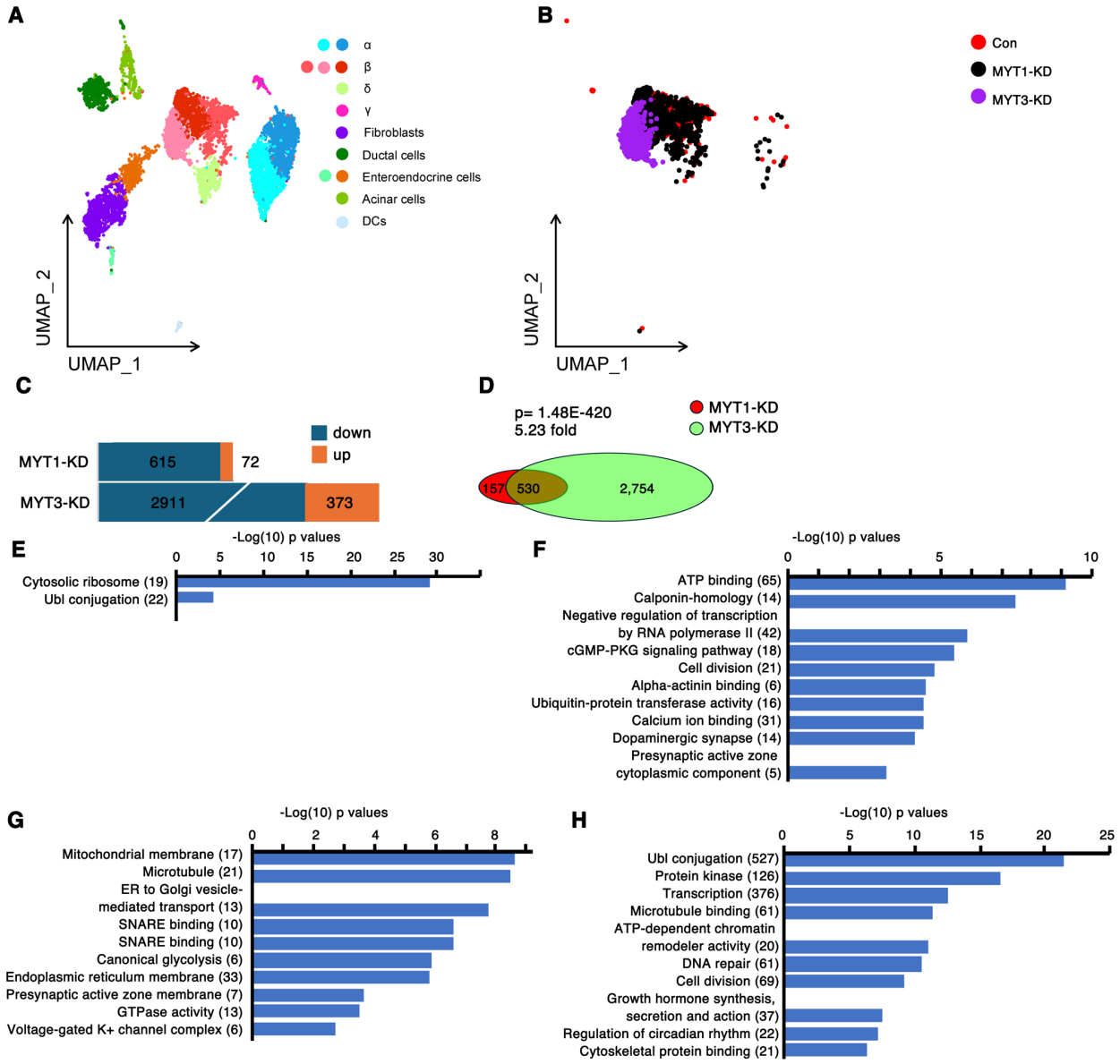

Fig. 5. Human MYT1- or MYT3-KD deregulates similar but distinct gene networks in β-cells. Freshly prepared PSIs were dissociated and used for InDrop scRNA-seq. One islet batch was used here. (A, B) UMAPs showing the separation of cells in PSIs, including all cells (A) or β-cells only (B). (C) The numbers of genes that were down- or upregulated with MYT1-KD or MYT3-KD cells. (D) The common and specific gene sets are de-regulated in MYT1- or MYT3-KD β-cells. (E, F) Pathways deregulated in MYT1-KD human β-cells either up- (E) or down-regulated (F) in mutants. (G, H) Pathways deregulated in MYT3-KD human β-cells, composed of up- (G) or down-regulated (H) genes in mutants. The number in parenthesis following each process refers to the number of genes discovered.

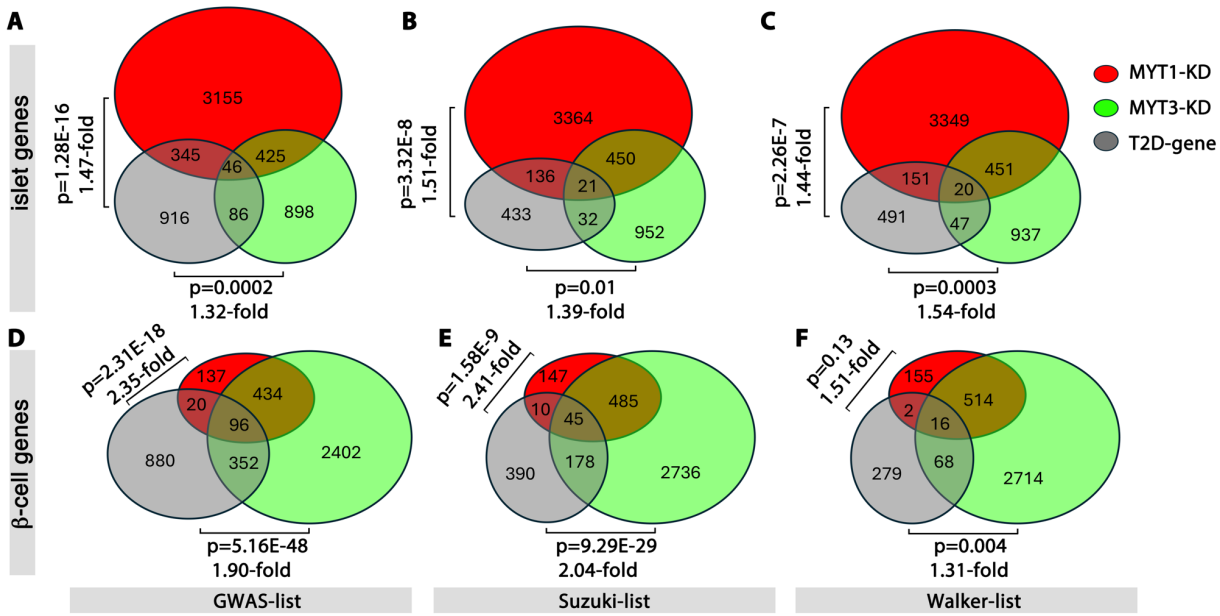

G

	Processes	p-values	genes
Suzuki-β	Brain development	7.53E-05	ROBO2, NEGR1, PTCH1, PTPN11, UNC5C, BPTF
	Chromatin regulator	0.002	SETD5, SMARCC1, JMJD1C, JARID2, HDAC9, BPTF
	Positive regulation of transcription by RNA Pol II	0.015	SMARCC1, ZFHX3, TCF12, GLIS3, IGF2, MAML3, GTF2I, BPTF
	Plasma membrane	0.037	ROBO2, MACF1, PATJ, NEGR1, PLEKHA1, ATP8B2, KCNH7, KCNB2, PTCH1, MAGI2, SCTR, SLC39A11, ITPR2, UNC5C, KSR2, LPP, DNM3, XKR6
GWAS-β	Chromatin regulator	3.27E-04	MORF4L1, SETD5, SMARCC1, PBRM1, JMJD1C, JARID2, ARID1B, HDAC9, BPTF
	Neurogenesis	1.15E-04	TTLL7, ROBO2, SMARCC1, MYT1L, MAGI2, TCF12, TNIK, ARID1B, ROBO1

Fig. 6. DEGs induced by MYT1- or MYT3-KD are enriched for T2D-associated genes. (A-C) Diagrams showing the numbers of overlapping genes between the T2D-associated genes and the DEGs induced by MYT1- or MYT3 KD. All genes with detectable expression in PSIs are included here. The fold of enrichment and p-values were calculated using hypergeometric tests. In (A), the GWAS gene list was used (Table S5). In (B), the Suzuki gene list was used (Table S7). In (C), the Walker gene list was used (Table S9). (D-F) The same as A-C, except that the background genes were only detected in β-cells (Tables S6, S8, and S10). (G) Biological processes enriched in the shared genes between T2D-associated genes, MYT1-KD-, and MYT3-KD-induced DEGS in β-cells from DAVID analysis.